Anti-Nogo-A Antibodies As a Potential Causal Therapy for Lower Urinary Tract Dysfunction after Spinal Cord Injury

Schneider, Marc P ; Sartori, Andrea M ; Ineichen, Benjamin V ; Moors, Selina ; Engmann, Anne K ; Hofer, Anna-Sophie ; Weinmann, Oliver ; Kessler, Thomas M ; Schwab, Martin E

Abstract: Loss of bladder control is common after spinal cord injury (SCI) and no causal therapies are available. Here we investigated whether function-blocking antibodies against the nerve-fiber growth inhibitory protein Nogo-A applied to rats with severe SCI could prevent development of neurogenic lower urinary tract dysfunction. Bladder function of rats with SCI was repeatedly assessed by urodynamic examination in fully awake animals. Four weeks after SCI, detrusor sphincter dyssynergia had developed in all untreated or control antibody-infused animals. In contrast, 2 weeks of intrathecal anti-Nogo-A antibody treatment led to significantly reduced aberrant maximum detrusor pressure during voiding and a reduction of the abnormal EMG high-frequency activity in the external urethral sphincter. Anatomically, we found higher densities of fibers originating from the pontine micturition center in the lumbosacral gray matter in the anti-Nogo-A antibody-treated animals, as well as a reduced number of inhibitory interneurons in lamina X. These results suggest that anti-Nogo-A therapy could also have positive effects on bladder function clinically. After spinal cord injury, loss of bladder control is common. Detrusor sphincter dyssynergia is a potentially life-threatening consequence. Currently, only symptomatic treatment options are available. First causal treatment options are urgently needed in humans. In this work, we show that function-blocking antibodies against the nerve-fiber growth inhibitory protein Nogo-A applied to rats with severe spinal cord injury could prevent development of neurogenic lower urinary tract dysfunction, in particular detrusor sphincter dyssynergia. Anti-Nogo-A therapy has entered phase II clinical trial in humans and might therefore soon be the first causal treatment option for neurogenic lower urinary tract dysfunction.

DOI: https://doi.org/10.1523/JNEUROSCI.3155-18.2019

As a Potential Causal Therapy for Lower Urinary Tract Dysfunction after Spinal Cord Injury. Journal of Neuroscience, 39(21):4066-4076.
DOI: https://doi.org/10.1523/JNEUROSCI.3155-18.2019

JNeurosci
THE JOURNAL OF NEUROSCIENCE

Research Articles: Development/Plasticity/Repair

Anti-Nogo-A antibodies as a potential causal therapy for lower urinary tract dysfunction after spinal cord injury

Marc P. Schneider[1,2], Andrea M. Sartori[1,2], Benjamin V. Ineichen[1], Selina Moors[1], Anne K. Engmann[1], Anna-Sophie Hofer[1], Oliver Weinmann[1], Thomas M. Kessler[2] and Martin E. Schwab[1]

[1]Brain Research Institute, University of Zürich, and Department of Health Sciences and Technology, ETH Zürich, 8057 Zürich, Switzerland

[2]Department of Neuro-Urology, Balgrist University Hospital, University of Zürich, 8008 Zürich, Switzerland

https://doi.org/10.1523/JNEUROSCI.3155-18.2019

Received: 17 December 2018

Accepted: 6 February 2019

Published: 22 March 2019

Author contributions: M.P.S., A.M.S., A.K.E., T.M.K., and M.E.S. designed research; M.P.S., A.M.S., B.V.I., S.M., A.K.E., A.-S.H., O.W., T.M.K., and M.E.S. performed research; M.P.S., A.K.E., T.M.K., and M.E.S. contributed unpublished reagents/analytic tools; M.P.S., A.M.S., O.W., and M.E.S. analyzed data; M.P.S. wrote the first draft of the paper; M.P.S., A.M.S., B.V.I., S.M., A.K.E., A.-S.H., O.W., T.M.K., and M.E.S. edited the paper; M.P.S. and M.E.S. wrote the paper.

Conflict of Interest: The authors declare no competing financial interests.

We thank Prof. P. Sawchenko and Dr. W.Vale from the Salk Institute for Biological Studies for giving us access to their CRF antibody. Furthermore, we would like to thank Pietro Morciano and Frank David from the information technology, as well as Stefan Giger, Hansjörg Kasper, Marco Tedaldi, and Martin Wieckhorst from the infrastructure team of the Brain Research Institute, University of Zürich, for their great support.

This study was supported by grants of the Swiss Continence Foundation, the Swiss National Science Foundation, a European Research Council (ERC) advanced grant (Nogorise) 5o MES, the Christopher and Dana Reeve Foundation, and the Santa Casa da Misericórdia de Lisboa (Prémio Mello e Castro - 2016). This work was awarded with the Swiss Continence Foundation Award at the 5th International Neuro-Urology Meeting, 25-28 January 2017, Zürich, Switzerland.

Corresponding address: Marc P. Schneider, Brain Research Institute, University of Zurich and Department of Health Science and Technology, Swiss Federal Institute of Technology Zurich, Winterthurerstrasse 190, 8057 Zürich, Switzerland, Mail: mpschneider@outlook.com

Cite as: J. Neurosci 2019; 10.1523/JNEUROSCI.3155-18.2019

Anti-Nogo-A antibodies as a potential causal therapy for lower urinary tract dysfunction after spinal cord injury

Marc P. Schneider[1,2,§,‡,*], Andrea M. Sartori[1,2,‡], Benjamin V. Ineichen[1], Selina Moors[1], Anne K. Engmann[1], Anna-Sophie Hofer[1], Oliver Weinmann[1], Thomas M. Kessler[2,¶] and Martin E. Schwab[1,¶]

‡ These authors share the first authorship

¶ These authors share the senior authorship

[1] Brain Research Institute, University of Zürich, and Department of Health Sciences and Technology, ETH Zürich, 8057 Zürich, Switzerland

[2] Department of Neuro-Urology, Balgrist University Hospital, University of Zürich, 8008 Zürich, Switzerland

[§] Present address: Department of Urology, Bern University Hospital, Inselspital, University of Bern, 3010 Bern, Switzerland

* Corresponding address: Marc P. Schneider
Brain Research Institute, University of Zurich
and Department of Health Science and Technology,
Swiss Federal Institute of Technology Zurich
Winterthurerstrasse 190
8057 Zürich, Switzerland
Mail: mpschneider@outlook.com

Abbreviation title: Anti-Nogo-A to treat NLUTD after SCI
Word count: abstract 149 words, introduction 630 words, discussion 1098 words, text 3408 words

Figures: 7

Keywords: Spinal cord injury, Nogo-A, urodynamics, rat, neuro-urology, neurogenic lower urinary tract dysfunction (NLUTD), CRF, interneurons, GABA

Competing interest statement

None of the funding organizations had a role in the design and conduct of the study, collection, management, analysis, and interpretation of the data, preparation, review, or approval of the manuscript, and decision to submit the manuscript for publication. MES is the co-founder and president of the board of NovaGo Therapeutics Inc..

Acknowledgements

We thank Prof. P. Sawchenko and Dr. W.Vale from the Salk Institute for Biological Studies for giving us access to their CRF antibody. Furthermore, we would like to thank Pietro Morciano and Frank David from the information technology, as well as Stefan Giger, Hansjörg Kasper, Marco Tedaldi, and Martin Wieckhorst from the infrastructure team of the Brain Research Institute, University of Zürich, for their great support.

Abstract

Loss of bladder control is common after spinal cord injury (SCI) and no causal therapies are available. Here we investigated if function blocking antibodies against the nerve fiber growth inhibitory protein Nogo-A applied to rats with severe SCI could prevent development of neurogenic lower urinary tract dysfunction. Bladder function of rats with SCI was repeatedly assessed by urodynamic examination in fully awake animals. Four weeks after SCI, detrusor sphincter dyssynergia had developed in all untreated or control antibody infused animals. In contrast, 2 weeks of intrathecal anti-Nogo-A-antibody treatment led to a significantly reduced aberrant maximum detrusor pressure during voiding and a reduction of the abnormal EMG high frequency activity in the external urethral sphincter. Anatomically, we found higher densities of fibers originating from the pontine micturition center in the lumbo-sacral grey matter in the anti-Nogo-A antibody treated animals, as well as a reduced number of inhibitory interneurons in *Lamina X*. These results suggest that anti-Nogo-A therapy could have positive effects on bladder function also clinically.

Significance Statement:

Bladder function is after spinal cord injury completely out of control. Detrusor sphincter dyssynergia, a potentially live threatening consequence, is greatly feared. Currently there are only symptomatic treatment options available and first causal treatment options are urgently needed in humans. In this work we show that function blocking antibodies against the nerve fiber growth inhibitory protein Nogo-A applied to rats with severe spinal cord injury could prevent development of neurogenic lower urinary tract dysfunction, in particular detrusor sphincter dyssynergia. Anti-Nogo-A therapy enters currently phase II clinical trial in humans and might therefore be soon the first causal treatment option for neurogenic lower urinary tract dysfunction.

Introduction

Many neurological diseases that affect descending tract systems, including spinal cord injury and multiple sclerosis, often lead to severe disturbances of bladder function. Detrusor sphincter dyssynergia (DSD)(Weld et al., 2000), which is defined by dys-synergic contractions of the external urethral sphincter during the voiding phase, is a life-threatening complication as it results in high intravesical pressure with subsequent urine reflux to the kidneys and, over years, can lead to kidney damage and eventually renal failure(Groen et al., 2016). Lower urinary tract dysfunction contributes in a major way to a decreased quality of life in the affected patients and therefore is one of the highest rehabilitation priorities(Simpson et al., 2012). However, only a few symptomatic treatment options are currently available including intermittent self-catheterization four to six times a day, antimuscarinic drugs, and intradetrusor onabotulinumtoxinA injections(Panicker et al., 2015). These treatments are at best symptomatic and come at the cost of frequent side effects such as urinary tract infections, or injuries to the urethra. Causal treatment options for neurogenic lower urinary tract dysfunctions, in particular DSD, are therefore urgently needed(Panicker et al., 2015).

The central neuronal circuits controlling lower urinary tract function are not yet fully understood. Storage and voiding of the urine are achieved by complex interactions between the somatic and the autonomic nervous system(de Groat et al., 2015). Although the storage reflex is mainly an intraspinal process(De Groat and Lalley, 1972), the initiation of voiding depends on supraspinal input from a nucleus located in the pons, the pontine micturition center (PMC)(Griffiths et al., 1990). The PMC-spinal projection neurons are excitatory and glutamatergic, with the peculiarity to also contain the neuropeptide corticotropin-releasing factor (CRF)(Verstegen et al., 2017).

These neurons send long-projecting axons to the lumbosacral cord and play a fundamental role in micturition. A lesion to the spinal cord disrupts the neural circuitry controlling the lower urinary tract function, and the neuro-urological consequences for the patient depend on the location and the extent of the injury. After a suprasacral SCI, the voluntary, supraspinal control of voiding is interrupted, leading to an initial acontractile bladder, causing urinary retention. After weeks to months, depending on the species, autonomic voiding slowly reappears and culminates in detrusor overactivity(de Groat et al., 1990), which was hypothesized to be the result of aberrant intraspinal plasticity with an important contribution by C-fibers(Cheng and de Groat, 2004). Although bladder contraction reappears over time, voiding is usually inefficient due to the simultaneous contraction of the external urethral sphincter together with the detrusor, a phenomenon that is known as detrusor-sphincter dyssynergia (DSD). DSD arises over time in the majority of patients with an incomplete or complete spinal cord injury, causing elevated intravesical pressures that, over time, put the upper urinary tract at risk(Bacsu et al., 2012; Groen et al., 2016).

Bladder function can be determined with high precision by urodynamic measurements, i.e. by simultaneously assessing the intravesical pressure and external urethral sphincter electromyography under fully awake conditions(Nosseir et al., 2007). This clinical protocol has recently been transferred and reproduced in intact and spinal cord injured rats(Schneider et al., 2015; Foditsch et al., 2018).

The CNS and myelin enriched membrane protein Nogo-A is a potent nerve fiber growth inhibitory protein, responsible in part for the low level spontaneous neuronal of regeneration and repair present in the adult mammalian CNS(Schwab, 2010; Schwab and Strittmatter, 2014). Neutralization by functionally blocking antibodies, genetic deletion of Nogo-A or blockade of Nogo-A receptors induces substantial

axonal regeneration, as well as enhanced neuronal plasticity and functional recovery after SCI or stroke in animal models(Liebscher et al., 2005; Schwab and Strittmatter, 2014; Wahl et al., 2014). It had been noted before that inhibition of Nogo-A in rats with large but incomplete spinal cord injuries using function blocking antibodies not only resulted in improved recovery of locomotion, but also led to an earlier restoration of independent voiding(Liebscher et al., 2005). However, a detailed urodynamic assessment of bladder function after SCI, assessing the potential of anti-Nogo-A antibodies as a potential therapy for DSD following spinal cord injury is so far missing. The present study aims at investigating the effects of anti-Nogo-A antibodies in the development of neurogenic lower urinary tract dysfunction, in particular DSD, following a large SCI in adult rats.

Materials and Methods

Rats: Adult female Lewis rats (LEW/OrlRj (Lewis), of 210 g ± 20 g body weight and 4 mts ± 1mts of age were purchased from Janvier, France. The rats were housed in groups of three to four per cage, and single housed after catheter implantation, food (rat chow) and water were provided ad libitum. Rats were maintained on a 12/12 h light/dark cycle (light on from 6:00 a.m. until 6:00 p.m). All experiments were approved by the Veterinary Office of the canton of Zürich, Switzerland (License nr. 19/2014) and were in accordance with the approved guidelines and regulations.

Catheter and electrodes implantation: All rats underwent initial preoperative handling and acclimatization to the urodynamic lab station followed by catheter and electrode implantation. Procedures were performed as described previously(Schneider et al., 2015; Foditsch et al., 2018). Briefly, rats were initially anesthetized in 5% Isoflurane (Piramal Healthcare) in air and maintained by an *i.m.* injection of Medetomidine (0.15 mg/kg Domitor, Orion Pharma), Midazolanum (2 mg/kg, Dormicum, Roche) and Fentanyl (5 µg/kg, Fentanyl, Kantonsapotheke University Hospital Zurich). Bladder catheters were inserted into the bladder dome and secured with a purse string suture. EMG electrodes were affixed to the fat tissue beside the external urethral sphincter and a ground electrode was sutured to the abdominal muscle. Catheter and wires were tunneled subcutaneously to the back of the neck, exteriorized, and lastly attached to an infusion harness (QC Single, SAI Infusion Technologies, USA).

Spinal cord injury: Rats were anesthetized as described above. In 41 animals, the T8 lamina was removed and the dorsal two thirds of the spinal cord were transected bilaterally microsurgically with iridectomy scissors, resulting in severe but incomplete

spinal cord injury. In 28 rats, the lower thoracic spinal cord was transected completely. Seventeen rats were left intact.

Osmotic pump implantation: Fifty-four spinal cord injured rats were implanted with intrathecal pumps for antibody delivery at the day of spinal cord injury. Following baseline urodynamic measurements, the rats were divided into four different groups: incomplete spinal cord injury with control antibody treatment (n= 17), complete spinal cord injury with control antibody treatment (n= 10), incomplete spinal cord injury with anti-Nogo-A antibody treatment (n= 16), complete spinal cord injury with anti-Nogo-A antibody treatment (n= 11). A pre-hoc power calculation (power = 80% and alpha = 0.05) indicated a minimal group size of n= 10 rats. The pump implantation procedure was performed as previously described(Ineichen et al., 2017). Briefly, immediately following the spinal cord injury, a second laminectomy at vertebrate level L2 was performed and a fine intrathecal catheter (32 Gauge, ReCathCo) was inserted into the subarachnoid space and pushed in cranial direction towards the lesion for 1 cm. The catheter was connected to an osmotic minipump (Alzet 2ML2) which continuously delivered over 14 days either an anti-Nogo-A antibody (mAB 11C7)(Oertle et al., 2003) or an inactive control antibody (Anti-BrdU, Serotec) into the intrathecal space (5 µl/h, 3 mg antibody/ml). In this way, 6 mg antibodies were applied in total over 14 days. Pump and catheter were removed 15-16 days post implantation under 5% Isoflurane (Piramal Healthcare) anesthesia and the skin was closed by sutures.

Urodynamic and external urethral sphincter EMG measurements: Procedures were performed as previously described(Schneider et al., 2015; Foditsch et al., 2018). Acclimatization of the rats to the urodynamic setup was performed before catheter and electrode implantation. Awake rats were positioned in a modified restrainer (modified from item # HLD-RM, Kent Scientific, Connecticut, USA) with a

hole situated under the orifice of the urethra. The restrainer was then placed in a modified Small Animal Cystometry Lab Station (Catamount Research and Development Inc.; St. Albans, Vermont, USA) with a scale below the funnel. The bladder catheter was attached to a syringe pump with an in-line pressure transducer and the electrodes were connected to an amplifier/converter. Saline was instilled (120 µL/min) and all parameters (pressure, scale, voltage) recorded simultaneously for at least 3 voiding cycles. Urodynamic measurements were performed during the light phase. For data assessment, the maximum voiding detrusor pressure was measured as the peak of the intravesical pressure during voiding (Figure 2 a). Voided volume was measured as the change in weight on the scale (assuming a density approaching 1). To serve as a measurement of the rigidity of the bladder wall, bladder compliance was calculated as the intravesical pressure increase (threshold detrusor pressure minus baseline detrusor pressure) divided by the voided volume. Urodynamic and behavioral assessments were performed on randomly number coded animals in a fully blinded fashion. Measurements were analyzed blinded using an adapted LabVIEW program.

EMG analysis: The external urethral sphincter (EUS)-EMG was bandpass filtered (2 Hz to 2 kHz). The frequency spectrogram was analyzed with a self-programmed application based on LabVIEW version 2012 (National Instruments, Austin, Texas, USA). The 45-second-long EMG signal is sliced into 4096 samples, a typical graphical representation of a spectral heatplot, of whom 3596 are overlapping (shift is 500 samples). After taking a hanning window of the signal, a fast Fourier transformation was generated. As a result, we obtained a power value for each frequency at every computed time point. Before graphic processing, the signal was up scaled by a multiplication factor to assure that the signal consists, after logarithmizing, mainly of positive values. The logarithmized signal was also scaled up

by factor 20. This signal was then plotted as color map with Jet Colormap. All frequencies above 500 Hz were neglected.

Quantification of high-frequency EUS-EMG activity was achieved by summing every high-frequency power value in the period of interest (before micturition = “r”, during micturition = “s”, or after micturition = “t”; Figure 1 j-k) and dividing it by the sum of every high-frequency power value in the whole period analyzed (labelled as “u”; Figure 1 j-k). Data are shown in percentage.

Perfusion fixation and tissue preparation: Rats were euthanized with an *i.p.* overdose of Pentobarbital (300mg/mL, Streuli Pharma AG). Animals were transcardially perfused first with 150 mL Ringer solution (B.Brown Medical) containing 1% Heparin (B. Brown Medical), followed by 300 mL of 4% Paraformaldehyde solution (Paraformaldehyde, PFA, Sigma-Aldrich) containing 5% sucrose and phosphate-buffered at pH 7.4. Spinal cords were dissected and post-fixed for 24 hrs at 4 °C in a solution containing 4 % paraformaldehyde and 15 % saturated picric acid for immunohistochemistry, or 4 % paraformaldehyde (Sigma-Aldrich Chemie GmbH, Buchs, Switzerland) in 0.1 M phosphate buffer pH 7.4 for RNAScope *in-situ* hybridization. Afterwards, spinal cords were transferred to 30% sucrose in 0.1 M phosphate buffer, pH 7.2 and stored for three days for cryo-protection. The tissue was embedded in Tissue-Tek OCT compound, frozen in 2-Methylbutane (Sigma-Aldrich Chemie GmbH, Buchs, Switzerland) cooled to -40 °C with liquid nitrogen and stored at -20 °C until further processing. For immunohistological analysis, 40-µm-thick L6-S1 spinal cord cross-sections were cut on a cryostat and collected on slides (Superfrost plus, Huberlab, Aesch, Switzerland), and kept at -20 °C until further processing. For *in-situ* hybridization analysis, 10-µm-thick L6-S1 spinal cord cross sections were collected free-floating in 4 °C cold 0.1 M phosphate buffer and kept in anti-freeze solution (15 % sucrose, 30 % ethylene

glycol in 50 mM phosphate buffer) at -20 °C until further processing. For histological lesion site analysis, T7 – T10 spinal cord sections were mounted on slides, dried on a heating plate at 60 °C for 10 min and then stored at -20 °C until further processing.

Assessment of lesion completeness: Coronal 40-µm cryostat serial sections of the injury site were manually reconstructed based on Nissl staining (Cresyl violet) in Photoshop software (Adobe, San José, USA). The percentage of spared white matter at the largest lesion extent was calculated. Initial comparison of Nissl staining and neurofilament 160 immunohistochemical staining showed a very high correlation between the two protocols (Figure 7 a-c). Low values of spared white matter were arduous to categorize into complete or incomplete groups based on the images. This, together with the fact that animals with a spared white matter below 3 % were equally distributed between the groups, lead to the conclusion that rats with a spared white matter below 3 % were considered to have a complete lesion.

Immunohistochemistry: On-slide spinal cord cross-sections were thawed for 10 min and then washed three times with 0.1 M phosphate buffer pH 7.2. Afterwards, they were permeabilized in TNB (0.5% TopBlock; LuBioScience in 0.1 M Tris) containing 0.2% Triton X-100 for 60 min at room temperature, and subsequently incubated with the primary antibody (rabbit-anti-CRF 1:400, Salk Institute, California) diluted in TNB and hypotonic 0.01 M phosphate buffer containing 0.05 % Triton X-100 at 4°C for 24 h. The sections were then washed three times in 0.1 M PBS for 10 min each and incubated with the secondary antibody (goat-anti-rabbit-Cy3 1:300, Jackson ImmunoResearch Laboratories). Stained sections were washed three times in 0.1 M phosphate buffer for 10 min each, finally incubated in 0.05 M Tris, pH 8.0, for 10 min, air-dried overnight at 4°C, and coverslipped with fluorescence mounting medium (Mowiol, Merck). Slides were stored at 4 °C upon imaging.

The specificity of the signal was assessed by omitting the incubation-step of the sections in the primary antibody.

RNAScope *in-situ* hybridization: Sequences of target probes, preamplifier, amplifier, and label probes are proprietary and commercially available (Advanced Cell Diagnosis). Here, we used probes against rat glycine transporter 2 ($GlyT_2$, Slc6a5), glutamic acid decarboxylase 2 (GAD_2), and vesicular glutamate transporter 2 ($vGluT_2$, Slc17a6).

Experimental protocols were according to Advanced Cell Diagnosis. Briefly, slides were thawed at room temperature for 15 min. Subsequently, slides were treated with ACD hydrogen peroxide for 10 min and washed twice in water for 2 min each, before incubation in ACD target retrieval buffer for 10 min at 98-100 °C. Slides were washed first in water and then in 100 % EtOH (Reuss Chemie, Taegerig, Switzerland), and then protease treatment was applied for 30 min at 40 °C in the ACD HybEZ^{TM} oven.

Subsequently, sections were incubated in a mix containing the three hybridization probes for 2 h at 40 °C. After washing the slides twice in ACD washing buffer, the three probes were amplified in a consecutive manner, with two washing-steps in ACD washing buffer in-between each amplification-step. Further amplification-steps were performed with HRP detecting the specific channel of the different probes, always with washing steps with ACD washing buffer in-between. The signals were developed with TSA Plus fluorescein, TSA Plus Cyanin3, and TSA Plus Cyanin5 (TSA Cy3, Cy5, TMR, Fluorescein Evaluation kit, PerkinElmer, USA) for the probe targeting $GlyT_2$, GAD_2, and $vGluT_2$, respectively. After the development of the last probe, sections were washed twice in ACD washing buffer and counterstained with ACD DAPI for 45 s at room temperature. Slides were coverslipped using fluorescence mounting medium (Mowiol, Merck) and let dry overnight in the dark. Afterwards, they were stored at 4 °C upon imaging.

Quantification of immunofluorescent signal: The CRF signal was quantified by imaging three randomly chosen sections with a confocal microscope (40x, Olympus FV1000, Olympus America). Microscope and laser parameters, such as laser intensity, were optimized during the first imaging and kept constant across all sections. Mosaic pictures were imaged and processed within Olympus FV1000 software. Maximum intensity projections were created, and pictures were exported in tiff format for investigation. Further analyses were performed with the Fiji image processing software (version 1.0, ImageJ, National Institutes of Health). Mean grey values for the regions of the dorsal horn, intermediolateral nucleus, and dorsal grey commissure were measured in the three sections and background intensities obtained from the central canal, where no signal is expected, were subtracted for each region. The values were normalized to the equivalent values of the intact animals.

Quantification of RNAScope in-situ hybridization: Five to seven sections per animal were imaged with a fluorescent microscope (20x, Zeiss Axio Scan.Z1, Zeiss). Three randomly chosen pictures were analyzed with Fiji and a custom-made MATLAB (2017b, The MathWorks Inc., Natick, USA) script. Briefly, the coordinates of each stained cell were retrieved within Fiji, and then used to plot the cells to a standardized spinal cord cross section template with MATLAB, thereby normalizing the analysis to potential tissue distortion. The number of $GlyT_2$-, GAD_2-, and $vGluT_2$-positive cells was calculated within the *laminae* 1, 2, 3, which reflect the dorsal horn, *laminae* 4,5, which comprehend the intermediolateral nucleus, and *lamina* X, comprising the dorsal grey commissure.

Statistical analysis: Data are reported as mean ± standard deviation (SD). Q-Q-plots were generated of all data and visually assessed, all data are assumed to be approximately normally distributed. For the comparison of the impact of spinal cord injury on bladder function by urodynamics, immunohistochemistry, and in-situ hybridization, data were analyzed with a one-way repeated-measures ANOVA followed by Bonferroni's post hoc testing. For comparison of unrelated samples, an unpaired t-test was used. The value of significance was considered at $p<0.05$. Pre-hoc power calculations were performed with alpha being 0.05 and a power of 80%. Statistical analyses were performed using STATA statistical software, version 14 (StataCorp, College Station, Texas, USA).

Results

Lower urinary tract dysfunction following spinal cord injury in adult rats

Animals were injured at day 0 and lower urinary tract function was assessed once a week for 4 weeks (Figure 1 a). On day 3-5 after the lesion, all rats in the SCI groups (complete and incomplete lesions) showed a complete initial paralysis of both hindlimbs as assessed by the BBB score (data not shown)(Basso et al., 1995). The T8 level bilateral partial transections interrupted between 2 and 55 % of the spinal cord white matter (Figure 7); spared white matter was mostly found in the ventral and ventro-lateral funiculi, often unilateral only. One week after injury, most rats of the incomplete lesion groups started to develop hind limb movements resulting into a BBB score > 10 three weeks post injury. Completely spinal cord injured animals showed a persisting severe impairment of hind limb function until the end of the experiment, i.e. up to four weeks post injury. The impairments observed in the rats are comparable to human SCI patients with American Spinal Injury Association (ASIA) impairment scale (AIS) A for the complete spinal cord injury group and AIS C for the incomplete SCI group (www.ais.emsci.org).

In all groups, bladder function was completely absent during the first week after injury and, very much in contrast to locomotor performance, showed only very limited spontaneous recovery. In both SCI groups, maximum detrusor pressure at 7 days post injury dropped significantly ($p < 0.05$) to about half of its value before SCI (Figure 1 b). Over the following 3 weeks, maximum detrusor pressure constantly increased, exceeding the baseline measurements at 4 weeks post injury. However, maximum detrusor pressure also increased in the intact group, reaching a value of 164 % of the baseline, a phenomenon that may be related to the chronic implantation of a bladder catheter. During voiding, maximum flow rates dropped to half of the pre-injury values

in both SCI groups (Figure 1 c). Bladder compliance was reduced in both SCI groups at 4 weeks post injury (Figure 1 d). Voiding time increased from 2 weeks post injury on (Figure 1 e). Voided volume was strongly and significantly reduced after injury, showing a certain degree of recovery but remaining significantly below baseline values in both injury groups until the end of the experiment (Figure 1 f). The intact group showed an increase of the voided volume over time compared to pre-lesion baseline. All these urodynamic findings are highly coherent to urodynamic observations made in human SCI patients and mirror the human acute and early chronic stages after spinal cord injury(Groen et al., 2016).

SCI induced changes in external urethral sphincter EMG activity: In intact rats, the EMG of the external urethral sphincter showed strong peak activity in the high frequency range (21-500Hz, representing mainly striated muscle activity (Solomonow et al., 1990)) at the high filling state immediately preceding voiding, as well as after voiding. High frequency activity was low during voiding (Figure 1 j and Figure 2 a, d), whereas in contrast, slow wave bursting activity (2-20Hz, representing mainly smooth muscle activity (Domino et al., 2017)) was prominent (Figure 1 j and Figure 2 a, d).

One week after injury, all spinal cord injured rats suffered from urinary retention and were unable to void by themselves. Urodynamic assessments confirmed this observation showing an acontractile bladder in all rats, which led to overflow incontinence once the bladder reached its maximum capacity (Figure 2 b, e).

Sixteen out of 17 rats with either complete or incomplete SCI developed DSD, starting 1-2 weeks after the lesion, characterized by tonic high frequency sphincter EMG activity (21-500Hz) during the voiding phase. This resulted in interrupted urine release and highly prolonged voiding phases (Figure 1 k and Figure 2 c, f). These

367 characteristic features again closely resemble the situation seen in severely spinal
368 cord injured human patients.

369 Urodynamic and external urethral sphincter parameters were not influenced by lesion
370 completeness: No significant differences were found in any urodynamic parameter
371 when the large, incomplete lesions and complete spinal cord injured animals were
372 compared (Figure 1 b-f). Also, we did not find differences in high frequency activity of
373 the external urethral sphincter EMG during voiding (Figure 1 h-i) between incomplete
374 and complete SCI groups.

375 **Effects of anti-Nogo-A antibody treatment on neurogenic lower urinary tract**
376 **dysfunction after incomplete spinal cord injury**

377 Anti-Nogo-A antibody therapy significantly reduced important urodynamic
378 abnormalities in incompletely spinal cord injured animals when compared to
379 incompletely lesioned animals treated with control antibody (Figure 3 a): Four weeks
380 after SCI, we observed significant changes towards more physiological values in
381 maximum detrusor pressure (Figure 3 b, $p= 0.01$), maximum flow rate (Figure 3 c, $p=$
382 0.05), compliance (Figure 3 d, $p= 0.006$), and voided volume (Figure 3 f, $p= 0.002$) of
383 anti-Nogo-A treated SCI animals. Voiding time four weeks after injury did not differ
384 between the treated and control group (Figure 3 e, $p > 0.05$). Anti-Nogo-A antibodies
385 also significantly reduced external urethral sphincter activity during voiding in
386 incompletely spinal cord injured animals compared to incompletely lesioned animals
387 treated with control antibody: Four weeks after SCI, we found a significant reduction
388 in the proportion of high frequency EMG values during voiding ($p= 0.002$) in the anti-
389 Nogo-A antibody treated animals when compared to control antibody treated spinal
390 cord injured animals (Figure 3 g).

391

Anti-Nogo-A treatment effects on neurogenic lower urinary tract dysfunction after complete *versus* incomplete spinal cord injury

We further investigated if the observed effect of anti-Nogo-A antibody therapy in incompletely spinal cord injured rats could be replicated in animals with a complete SCI (Figure 4 a). Anti-Nogo-A antibody treated animals showed again a trend towards a more pronounced treatment effect in incompletely spinal cord injured animals compared to incompletely lesions animals treated with control. Several of the urodynamic abnormalities were reduced starting 2-3 weeks after SCI (Figure 4 b-g). Four weeks after SCI, the anti-Nogo-A antibody treated group showed a reduction in maximum detrusor pressure (50%, Figure 4 b), maximum flow rate (32%, Figure 4 c), compliance (46%, Figure 4 d), voiding time (62 %, Figure 4 e), and voided volume (34%, Figure 4 f) when compared to the control antibody treated group. The proportion of high frequency EMGs during voiding showed the biggest change; it was decreased by 73% in the anti-Nogo-A treated animals (Figure 4 g). Very much in contrast to these group-differences in the incompletely lesioned rats, no effect of anti-Nogo-A therapy on lower urinary tract function was observed in animals with a complete SCI (Figure 4 b-g). However, no statistical testing was performed in this experiment due to the restricted number of animals per group.

411 **Neuroanatomical changes in the lumbo-sacral spinal cord after injury and**
412 **anti-Nogo-A antibody treatment**

413 The neuropeptide CRF is highly enriched in PMC neurons projecting to the lumbo-
414 sacral spinal cord(Valentino et al., 1994; Verstegen et al., 2017). Immunofluorescent
415 stainings for CRF in cross sections of the L6-S1 spinal cord revealed three main
416 target regions innervated by CRF-positive fibers: *lamina II* of the dorsal horn (Lam II),
417 the intermediolateral nucleus (IML), and *Lamina X* of the ventral grey matter (Lam X)
418 (Figure 5 a). Interestingly, the IML contains the preganglionic autonomic
419 motoneurons responsible for bladder contraction(De Groat and Ryall, 1968;
420 Nadelhaft and Booth, 1984), while the Lam X contains interneurons that were shown
421 to modulate the activity of somatic motoneurons innervating the bladder and external
422 urethral sphincter(Marson, 1997; Nadelhaft and Vera, 2001). The observed CRF
423 signal in Lam II is believed to originate from innervating peripheral sensory
424 fibers(Skofitsch et al., 1985; Kim et al., 2011), since previous anterograde tracings
425 from the PMC did not result in labelling of this region(Verstegen et al., 2017). Four
426 weeks after incomplete SCI, animals treated with control antibodies showed a strong,
427 significant decrease in CRF-positive innervation of Lam X compared to non-injured
428 animals ($p=0.004$). In contrast, the density of CRF-positive fibers and terminals in this
429 region in the injured anti-Nogo-A antibody treated rats was not different from that of
430 intact rats ($p=0.99$) but was significantly higher than that of the control antibody spinal
431 cord injured animals (Figure 5 b-d/ k; $p=0.009$). In the IML region, both injury groups
432 showed a reduced CRF-positive fiber density compared to intact animals (Figure 5 e-
433 g, m; $p=0.0001$ and 0.0006, respectively). Anti-Nogo-A treated rats showed a trend
434 for higher values (Fig. 5). In contrast, no difference was observed between the two
435 injury groups ($p= 0.33$) in the Lam II CRF-innervation, which significantly decreased

436 in both spinal cord injured groups when compared to intact rats (Figure 5 h-j/ l;
437 p=0.02).

438 We further analyzed the numbers of glycinergic, GABAergic, and glutamatergic
439 interneurons located in the segments L6-S1 of the spinal cord using *in-situ*
440 hybridization for the respective cell type specific markers *GLYT2*, *GAD2* and
441 *VGLUT2* mRNAs. No differences in the number of glycinergic cells expressing
442 *GLYT2* mRNA were observed between intact animals and rats with large but
443 incomplete SCIs treated with either control or anti-Nogo-A antibodies in none of the
444 regions analyzed, i.e. *Laminae* I-III, IV-V, and X (Figure 6 a, e, f). The number of
445 GABAergic, *GAD2* mRNA-positive cells showed a trend towards a decrease in cell
446 number in all areas analyzed. However, only the dorsal grey commissure area
447 showed a small but significant reduction in *GAD2*-positive neurons in the spinal cord
448 injured, control antibody treated rats when compared to intact animals (p= 0.04).
449 Interestingly, this reduction in cell-number was not present in the anti-Nogo-A treated
450 SCI group (Figure 6 b/g). Furthermore, we did not observe any difference between
451 groups in the number of glutamatergic, *VGLUT2*-positive neurons in neither *laminae*
452 *I-III*, *IV-V*, nor *X* (Figure 6 c, e, i).

453

Discussion

A massive increase in EMG activity of the external urethral sphincter during the voiding phase was the most prominent change observed using urodynamic measurements in adult rats with either an incomplete or complete lesion in the low thoracic spinal cord. This wrongly timed increase in EUS-EMG activity is a hallmark for DSD, which is defined by a dys-synergistic contraction of the external urethral sphincter during voiding resulting in increased bladder pressure and therefore compromised voiding. In humans, this often results in urinary reflux to the kidneys and over time to life-threatening kidney damage(Panicker et al., 2015). Interestingly, like in patients with spinal cord injury, the characteristic DSD features in rats developed over time, i.e. at 2-4 weeks after injury, which is very much in line with the human condition (1-6 months in humans(Bywater et al., 2018)). Our findings in rats are therefore highly translational and comparable to data from human SCI patients(Weld et al., 2000; Fowler et al., 2008; Schops et al., 2015). Intrathecal administration of anti-Nogo-A antibodies for 2 weeks after a large but incomplete T8 SCI resulted in a reduction of the impairment of several key urodynamic functions at 4 weeks post lesion: among others, the EMG overactivity of the external urethral sphincter during voiding recovered nearly back to pre-lesion baseline levels. This was in great contrast to control antibody treated SCI animals. However, no treatment effect was observed in animals with a complete spinal cord injury treated with anti-Nogo-A antibody. These findings indicate a crucial role of the remaining descending ventral tract fibers (4-38% of white matter sparring in our study) in the anti-Nogo-A treatment enhanced restoration of bladder function.

In human spinal cord injured patients, the development of neurogenic lower urinary tract dysfunction after spinal cord injury follows a typical time course, which is

479 characterized by an initial phase of detrusor and sphincter muscle inactivity (flaccid
480 bladder), resulting in incontinence and high post void residuals(Panicker et al., 2015).
481 A very similar situation was encountered in our rats in all the experimental SCI
482 groups at 7 days post injury. Absence of descending control and spinal shock are the
483 most likely reasons for this condition. Detrusor overactivity and simultaneous
484 abnormal contractions of the external urethral sphincter during voiding(Abrams et al.,
485 2002) then lead to increased intravesical pressure. In our animal model, the
486 incomplete thoracic SCI resulted in the development of characteristic DSD features
487 within the first 4 weeks following injury. Impairment of most of the urodynamic and
488 EUS-EMG parameters was much more pronounced after an incomplete lesion than
489 after a complete SCI. This finding points to an important role of spared descending
490 fibers and their potential detrimental, spontaneous plastic changes after partial injury
491 for the initial development of DSD.

492 Intrathecal delivery of function blocking anti-Nogo-A antibodies, which have been
493 shown to promote nerve fiber sprouting and regeneration in the adult mammalian
494 CNS(Liebscher et al., 2005; Lindau et al., 2014), for the first two weeks after the
495 lesion had a strong positive effect on the recovery of bladder function. Several of the
496 key urodynamic and electrophysiological parameters showed significant and
497 pronounced improvement in the anti-Nogo-A compared to the control antibody
498 treated SCI group. Most strikingly, the anti-Nogo-A antibody treatment led to a
499 pronounced recovery of the physiological external urethral sphincter function during
500 voiding. Anti-Nogo-A antibody treatment has been shown to induce regeneration and
501 sprouting of the corticospinal tract(Liebscher et al., 2005; Freund et al., 2006) and
502 restoration of the serotonergic projection density(Mullner et al., 2008) after large but
503 incomplete SCI in several species, including macaque monkeys.
504 Immunohistochemical staining against the neuropeptide CRF allowed us to

505 specifically visualize descending projections from the PMC to the lumbosacral spinal
506 cord(Skofitsch et al., 1985; Kim et al., 2011). In line with existing literature, animals
507 with a SCI showed a massive decrease in CRF-positive fibers in the lumbosacral
508 spinal grey matter at 4 weeks after injury(Studeny and Vizzard, 2005). Interestingly,
509 animals that were treated with the anti-Nogo-A antibodies during the first two weeks
510 after injury showed CRF fiber densities comparable to intact rats in Lam X, but not in
511 Lam II or in the IML, where the PMC fiber loss was comparable to the control
512 antibody treated SCI rats. This suggests that, in the anti-Nogo-A treated animals, the
513 spared descending fibers from the PMC sprouted below the level of the injury in a
514 specific target region, Lam X, thereby restoring functional, supraspinal input from the
515 key bladder control system located in the brainstem. Keller and colleagues recently
516 showed that in addition to the CRF-positive neurons, the PMC contains an additional
517 population of neurons that is positive for the estrogen receptor 1 alpha. This estrogen
518 receptor 1 alpha-positve nueornal population in the PMC is crucial for the correct
519 function of the external urethral sphincter and thereby for voluntary control of
520 micturition(Keller et al., 2018). Thus, CRF positive fibers might not be the only key
521 players in the observed recovery of lower urinary tract function following anti-Nogo-A
522 therapy. In fact, a number of additional changes in the circuitry underlying the control
523 of bladder function will be enhanced by the temporary neutralization of the neurite
524 growth inhibitory factor Nogo-A and thereby might contribute to the reconfiguration of
525 the bladder control on spinal and supraspinal levels(Bareyre et al., 2004; Filli et al.,
526 2014). Our results are also in line with an earlier study which found that rats with
527 slightly smaller incomplete lesions recovered functional bladder control earlier if
528 treated with anti-Nogo-A antibodies(Liebscher et al., 2005).

529 Former studies investigating the neural circuits involved in lower urinary tract function
530 showed that the PMC projects to GABAergic and glycinergic interneurons in the

lumbosacral cord(Blok and Holstege, 2000; Sie et al., 2001), and that a SCI causes a downregulation of glycine and GABA in the spinal cord and lumbosacral dorsal root ganglia of rats(Miyazato et al., 2003; Miyazato et al., 2008a). Furthermore, spinal cord injured animals affected by detrusor overactivity and DSD showed some degrees of recovery after dietary supplementation of glycine, or intrathecal application of $GABA_A$ or $GABA_B$ agonists(Miyazato et al., 2005; Miyazato et al., 2008b). These results indicate that inhibitory intraspinal connectivity is essential to coordinate bladder and sphincter function. Our results also suggest that these interneuron populations in the lumbosacral cord tend to decrease in number after injury, possibly due to a lack of descending inputs and therefore proper synaptic innervation. The decrease in numbers of GABAergic interneurons was dampened in the animals treated with anti-Nogo-A antibodies. This can most likely be explained by anti-Nogo-A treatment enhancing the sprouting of spared descending fibers below the injury site, thereby restoring critical synaptic inputs to the interneurons.

A human phase I safety and tolerability trial with intrathecal application of anti-Nogo-A antibodies in acutely spinal cord injured patients was concluded successfully(Kucher et al., 2018). Phase two randomized controlled European multicenter trial testing for upper limb motor recovery in acute tetraplegic patients is currently on-going (https://nisci-2020.eu). Bladder parameters will be monitored as part of the panel of secondary read-outs in this trial. Data addressing potential beneficial effects of Nogo-A suppression after SCI in humans should therefore become available soon.

Acknowledgements

We thank Prof. P. Sawchenko and Dr. W.Vale from the Salk Institute for Biological Studies for giving us access to their CRF antibody. Furthermore, we would like to thank Pietro Morciano and Frank David from the information technology, as well as Stefan Giger, Hansjörg Kasper, Marco Tedaldi, and Martin Wieckhorst from the infrastructure team of the Brain Research Institute, University of Zürich, for their great support.

Funding

This study was supported by grants of the Swiss Continence Foundation, the Swiss National Science Foundation, a European Research Council (ERC) advanced grant (Nogorise) 5o MES, the Christopher and Dana Reeve Foundation, and the Santa Casa da Misericórdia de Lisboa (Prémio Mello e Castro - 2016).

This work was awarded with the Swiss Continence Foundation Award at the 5th International Neuro-Urology Meeting, 25-28 January 2017, Zürich, Switzerland.

Author contributions

MPS, AMS, TMK, and MES conceived and planned the experiments. MPS, AMS, BVI, SM, AKE, and ASH carried out the experiments. MPS, AMS, SM, and OW contributed to sample preparation. MPS, AMS, BVI, AKE, TMK, and MES contributed to the interpretation of the results. MPS, AMS and MES wrote the manuscript. All authors provided critical feedback and helped shape the research, analysis and manuscript.

Competing interest statement

None of the funding organizations had a role in the design and conduct of the study, collection, management, analysis, and interpretation of the data, preparation, review, or approval of the manuscript, and decision to submit the manuscript for publication. MES is the co-founder and president of the board of NovaGo Therapeutics Inc..

Data and materials availability

Main data is included in the Manuscript. All additional data are accessible through mail contact to the corresponding author.

References

Abrams P, Cardozo L, Fall M, Griffiths D, Rosier P, Ulmsten U, van Kerrebroeck P, Victor A, Wein A (2002) The standardisation of terminology of lower urinary tract function: report from the Standardisation Sub-committee of the International Continence Society. Neurourology and urodynamics 21:167-178.

Bacsu CD, Chan L, Tse V (2012) Diagnosing detrusor sphincter dyssynergia in the neurological patient. BJU international 109 Suppl 3:31-34.

Bareyre FM, Kerschensteiner M, Raineteau O, Mettenleiter TC, Weinmann O, Schwab ME (2004) The injured spinal cord spontaneously forms a new intraspinal circuit in adult rats. Nature neuroscience 7:269-277.

Basso DM, Beattie MS, Bresnahan JC (1995) A sensitive and reliable locomotor rating scale for open field testing in rats. Journal of neurotrauma 12:1-21.

Blok BFM, Holstege G (2000) The pontine micturition center in rat receives direct lumbosacral input. An ultrastructural study. Neuroscience Letters 282:29-32.

Bywater M, Tornic J, Mehnert U, Kessler TM (2018) Detrusor Acontractility after Acute Spinal Cord Injury-Myth or Reality? The Journal of urology 199:1565-1570.

Cheng CL, de Groat WC (2004) The role of capsaicin-sensitive afferent fibers in the lower urinary tract dysfunction induced by chronic spinal cord injury in rats. Experimental neurology 187:445-454.

De Groat WC, Ryall RW (1968) The identification and characteristics of sacral parasympathetic preganglionic neurones. The Journal of physiology 196:563-577.

De Groat WC, Lalley PM (1972) Reflex firing in the lumbar sympathetic outflow to activation of vesical afferent fibres. The Journal of physiology 226:289-309.

de Groat WC, Griffiths D, Yoshimura N (2015) Neural control of the lower urinary tract. Comprehensive Physiology 5:327-396.

de Groat WC, Kawatani M, Hisamitsu T, Cheng CL, Ma CP, Thor K, Steers W, Roppolo JR (1990) Mechanisms underlying the recovery of urinary bladder function following spinal cord injury. J Auton Nerv Syst 30 Suppl:S71-77.

Domino M, Pawlinski B, Gajewski Z (2017) Biomathematical pattern of EMG signal propagation in smooth muscle of the non-pregnant porcine uterus. PloS one 12:e0173452.

Filli L, Engmann AK, Zorner B, Weinmann O, Moraitis T, Gullo M, Kasper H, Schneider R, Schwab ME (2014) Bridging the gap: a reticulo-propriospinal detour bypassing an incomplete spinal cord injury. The Journal of neuroscience : the official journal of the Society for Neuroscience 34:13399-13410.

Foditsch EE, Roider K, Sartori AM, Kessler TM, Kayastha SR, Aigner L, Schneider MP (2018) Cystometric and External Urethral Sphincter Measurements in Awake Rats with Implanted Catheter and Electrodes Allowing for Repeated Measurements. Journal of visualized experiments : JoVE.

Fowler CJ, Griffiths D, de Groat WC (2008) The neural control of micturition. Nature reviews Neuroscience 9:453-466.

Freund P, Schmidlin E, Wannier T, Bloch J, Mir A, Schwab ME, Rouiller EM (2006) Nogo-A-specific antibody treatment enhances sprouting and functional recovery after cervical lesion in adult primates. Nature medicine 12:790-792.

Griffiths D, Holstege G, Dalm E, Wall HD (1990) Control and coordination of bladder and urethral function in the brainstem of the cat. Neurourology and urodynamics 9:63-82.

Groen J, Pannek J, Castro Diaz D, Del Popolo G, Gross T, Hamid R, Karsenty G, Kessler TM, Schneider M, t Hoen L, Blok B (2016) Summary of European Association of Urology (EAU) Guidelines on Neuro-Urology. European urology 69:324-333.

Ineichen BV, Schnell L, Gullo M, Kaiser J, Schneider MP, Mosberger AC, Good N, Linnebank M, Schwab ME (2017) Direct, long-term intrathecal application of therapeutics to the rodent CNS. Nature protocols 12:104-131.

637 Keller JA, Chen J, Simpson S, Wang EH, Lilascharoen V, George O, Lim BK, Stowers L (2018) Voluntary
638 urination control by brainstem neurons that relax the urethral sphincter. Nature
639 neuroscience 21:1229-1238.
640 Kim EH, Ryu DH, Hwang S (2011) The expression of corticotropin-releasing factor and its receptors in
641 the spinal cord and dorsal root ganglion in a rat model of neuropathic pain. Anatomy & cell
642 biology 44:60-68.
643 Kucher K, Johns D, Maier D, Abel R, Badke A, Baron H, Thietje R, Casha S, Meindl R, Gomez-Mancilla
644 B, Pfister C, Rupp R, Weidner N, Mir A, Schwab ME, Curt A (2018) First-in-Man Intrathecal
645 Application of Neurite Growth-Promoting Anti-Nogo-A Antibodies in Acute Spinal Cord Injury.
646 Neurorehabilitation and neural repair 32:578-589.
647 Liebscher T, Schnell L, Schnell D, Scholl J, Schneider R, Gullo M, Fouad K, Mir A, Rausch M, Kindler D,
648 Hamers FP, Schwab ME (2005) Nogo-A antibody improves regeneration and locomotion of
649 spinal cord-injured rats. Annals of neurology 58:706-719.
650 Lindau NT, Banninger BJ, Gullo M, Good NA, Bachmann LC, Starkey ML, Schwab ME (2014) Rewiring
651 of the corticospinal tract in the adult rat after unilateral stroke and anti-Nogo-A therapy.
652 Brain : a journal of neurology 137:739-756.
653 Marson L (1997) Identification of central nervous system neurons that innervate the bladder body,
654 bladder base, or external urethral sphincter of female rats: a transneuronal tracing study
655 using pseudorabies virus. The Journal of comparative neurology 389:584-602.
656 Miyazato M, Sugaya K, Nishijima S, Ashitomi K, Hatano T, Ogawa Y (2003) Inhibitory effect of
657 intrathecal glycine on the micturition reflex in normal and spinal cord injury rats.
658 Experimental neurology 183:232-240.
659 Miyazato M, Sugaya K, Nishijima S, Ashitomi K, Morozumi M, Ogawa Y (2005) Dietary glycine inhibits
660 bladder activity in normal rats and rats with spinal cord injury. The Journal of urology
661 173:314-317.
662 Miyazato M, Sasatomi K, Hiragata S, Sugaya K, Chancellor MB, de Groat WC, Yoshimura N (2008a)
663 GABA receptor activation in the lumbosacral spinal cord decreases detrusor overactivity in
664 spinal cord injured rats. The Journal of urology 179:1178-1183.
665 Miyazato M, Sasatomi K, Hiragata S, Sugaya K, Chancellor MB, de Groat WC, Yoshimura N (2008b)
666 Suppression of detrusor-sphincter dysynergia by GABA-receptor activation in the
667 lumbosacral spinal cord in spinal cord-injured rats. American journal of physiology
668 Regulatory, integrative and comparative physiology 295:R336-342.
669 Mullner A, Gonzenbach RR, Weinmann O, Schnell L, Liebscher T, Schwab ME (2008) Lamina-specific
670 restoration of serotonergic projections after Nogo-A antibody treatment of spinal cord injury
671 in rats. The European journal of neuroscience 27:326-333.
672 Nadelhaft I, Booth AM (1984) The location and morphology of preganglionic neurons and the
673 distribution of visceral afferents from the rat pelvic nerve: a horseradish peroxidase study.
674 The Journal of comparative neurology 226:238-245.
675 Nadelhaft I, Vera PL (2001) Separate urinary bladder and external urethral sphincter neurons in the
676 central nervous system of the rat: simultaneous labeling with two immunohistochemically
677 distinguishable pseudorabies viruses. Brain Res 903:33-44.
678 Nosseir M, Hinkel A, Pannek J (2007) Clinical usefulness of urodynamic assessment for maintenance
679 of bladder function in patients with spinal cord injury. Neurourology and urodynamics
680 26:228-233.
681 Oertle T, van der Haar ME, Bandtlow CE, Robeva A, Burfeind P, Buss A, Huber AB, Simonen M, Schnell
682 L, Brosamle C, Kaupmann K, Vallon R, Schwab ME (2003) Nogo-A inhibits neurite outgrowth
683 and cell spreading with three discrete regions. The Journal of neuroscience : the official
684 journal of the Society for Neuroscience 23:5393-5406.
685 Panicker JN, Fowler CJ, Kessler TM (2015) Lower urinary tract dysfunction in the neurological patient:
686 clinical assessment and management. The Lancet Neurology 14:720-732.
687 Schneider MP, Hughes FM, Jr., Engmann AK, Purves JT, Kasper H, Tedaldi M, Spruill LS, Gullo M,
688 Schwab ME, Kessler TM (2015) A novel urodynamic model for lower urinary tract assessment
689 in awake rats. BJU international 115 Suppl 6:8-15.

690 Schops TF, Schneider MP, Steffen F, Ineichen BV, Mehnert U, Kessler TM (2015) Neurogenic lower
691 urinary tract dysfunction (NLUTD) in patients with spinal cord injury: long-term urodynamic
692 findings. BJU international 115 Suppl 6:33-38.
693 Schwab ME (2010) Functions of Nogo proteins and their receptors in the nervous system. Nature
694 reviews Neuroscience 11:799-811.
695 Schwab ME, Strittmatter SM (2014) Nogo limits neural plasticity and recovery from injury. Current
696 opinion in neurobiology 27:53-60.
697 Sie JA, Blok BF, de Weerd H, Holstege G (2001) Ultrastructural evidence for direct projections from
698 the pontine micturition center to glycine-immunoreactive neurons in the sacral dorsal gray
699 commissure in the cat. The Journal of comparative neurology 429:631-637.
700 Simpson LA, Eng JJ, Hsieh JT, Wolfe DL (2012) The health and life priorities of individuals with spinal
701 cord injury: a systematic review. Journal of neurotrauma 29:1548-1555.
702 Skofitsch G, Zamir N, Helke CJ, Savitt JM, Jacobowitz DM (1985) Corticotropin releasing factor-like
703 immunoreactivity in sensory ganglia and capsaicin sensitive neurons of the rat central
704 nervous system: colocalization with other neuropeptides. Peptides 6:307-318.
705 Solomonow M, Baten C, Smit J, Baratta R, Hermens H, D'Ambrosia R, Shoji H (1990) Electromyogram
706 power spectra frequencies associated with motor unit recruitment strategies. Journal of
707 applied physiology (Bethesda, Md : 1985) 68:1177-1185.
708 Studeny S, Vizzard MA (2005) Corticotropin-releasing factor (CRF) expression in postnatal and adult
709 rat sacral parasympathetic nucleus (SPN). Cell Tissue Res 322:339-352.
710 Valentino RJ, Page ME, Luppi PH, Zhu Y, Van Bockstaele E, Aston-Jones G (1994) Evidence for
711 widespread afferents to Barrington's nucleus, a brainstem region rich in corticotropin-
712 releasing hormone neurons. Neuroscience 62:125-143.
713 Verstegen AMJ, Vanderhorst V, Gray PA, Zeidel ML, Geerling JC (2017) Barrington's nucleus:
714 Neuroanatomic landscape of the mouse "pontine micturition center". The Journal of
715 comparative neurology 525:2287-2309.
716 Wahl AS, Omlor W, Rubio JC, Chen JL, Zheng H, Schröter AG, M. , Weinmann O, Kobayashi K,
717 Helmchen F, Ommer B, Schwab ME (2014) Asynchronous therapy restores motor control by
718 rewiring of the rat corticospinal tract after stroke. Science 344.
719 Weld KJ, Graney MJ, Dmochowski RR (2000) Clinical significance of detrusor sphincter dyssynergia
720 type in patients with post-traumatic spinal cord injury. Urology 56:565-568.

721

722

Figure legends

Figure 1: **Time-course of lower urinary tract dysfunction after SCI**. – **a**. Study design. **b-f.** Urodynamic parameters change after spinal cord injury. **b.** Maximum detrusor pressure [cmH_2O]; **c.** Maximum flow rate [mL/s]; **d.** Bladder compliance [mL/cmH_2O]; **e.** Voiding time [s]; **f.** Voided volume [mL]. **g-k.** External urethral sphincter EMG analysis before and 1, 2, 3, and 4 weeks after incomplete or complete spinal cord injury. **g**. EMG power spectrum shows highest percentual power for the high frequencies (21-500 Hz) before voiding in intact rats. **h.** After a large but incomplete spinal cord injury, the high frequency power activity (21-500Hz) of the external urethral sphincter shifts to the micturition phase starting at d.7, a condition typical for DSD. **i.** Similar but less pronounced shift in complete SCI rats. **j**. EUS-EMG Spectrogram of one voiding cycle of an intact rat showing increased high frequency power activity (21-500 Hz, bigger quadrant) before micturition, followed by slow wave bursting activity (1-20 Hz, smaller quadrant) during micturition. **k**. EUS-EMG spectrogram of one voiding cycle of an incompletely spinal cord injured rat four weeks after spinal cord injury. Percentual power in g-i was calculated dividing the power of high-frequencies in the period of interest (before = r; during = s; after = t) by the whole analyzed period (u). Statistical testing: data of intact and both complete and incomplete spinal cord injury were analyzed with a one-way repeated-measures ANOVA followed by Bonferroni's post hoc testing; *= $p<0.05$; **= $p<0.01$ and ***= $p<0.001$.

Figure 2: **Bladder pressure, voided urine and external urethral sphincter EMGs before (intact) and 7 and 28 days after incomplete spinal cord injury. DSD is fully developed at 4 weeks after injury.** - **a**., **d.:** 40 min. (2200 sec.) and 1min. (60 sec.) windows of a

representative urodynamic tracing from an intact rat with bladder catheter and external urethral sphincter EMG showing filling/voiding cycles. Top panels: bladder pressure, middle panels: urine secreted (weight), bottom panels: external urethral sphincter EMG. Lowest panel: Heat plot of EMG frequency spectrogram where red represents a high power of the corresponding frequency at the current time point and blue represents low power. **b**., **e.** Spinal cord injured rat at one week after injury shows a flaccid bladder with continuous flow of urine and absent sphincter activity **c**., **f.** Typical characteristics of DSD at 4 weeks after injury. During the filling phase there are non-voiding contractions with increasing magnitude as well as an increase in EUS-EMG activity during voiding.

Figure 3: Anti-Nogo-A effects on lower urinary tract function in incomplete spinal cord injury assessed by urodynamics. - **a**. Study design; **b**. Maximum detrusor pressure [cmH2O]; **c**. Maximum flow rate [mL/s]; **d**. Bladder compliance [mL/cmH2O]; **e.** Voiding time [s]; **f**. Voided volume [mL]; **g**. EMG activity during voiding (period s, Figure 1 j-k) in comparison to the whole period analyzed (period u, Figure 1 j-k) [%]. Statistical testing: data of anti-Nogo-A antibody treated rats and control antibody treated rats were analyzed with an unpaired students t-test; *= $p<0.05$; **= $p<0.01$ and ***= $p<0.001$. Red dashed line reflects the values of intact animals.

Figure 4: Anti-Nogo-A effects on lower urinary tract function in incomplete versus complete spinal cord injury assessed by urodynamics. - **a**. Study design; **b**. Maximum detrusor pressure [cmH2O]; **c**. Maximum flow rate [mL/s]; **d**. Bladder compliance [mL/cmH2O]; **e.** Voiding time [s]; **f**. Voided volume [mL]; **g**. EMG activity during voiding (period s, Figure 1 j-k) in comparison to the whole period analyzed (period u, Figure 1 j-k) [%]; No statistical testing was performed on this study.

772

773 **Figure 5: Innervation of lumbosacral spinal cord by CRF-positive fibers including bulbo-**
774 **spinal fibers from the pontine micturition center at 28 days after injury. - a.** In intact rats
775 immunofluorescent CRF-positive fibers and terminals are concentrated in dorsal horn *lamina*
776 *II* (Lam II), the intermediolateral column (IML), and *Lamina X* (Lam X). **b-j.** High magnification
777 (40x) of **b-d.** Lamina X, **e-g.** Intermediolateral column, and **h-j.** dorsal horn in intact, spinal
778 cord injured control antibody treated (Ctr Ab) and injured anti-Nogo-A antibody treated rats.
779 **k-m.** Relative optical density quantitation for CRF in Lam X, IML, and Lam II. Data are
780 presented as means ± SD. Scale bar is 100 μm in **a.** and 20 μm in **b-j.**; ns = not significant; *=
781 $p<0.05$; **= $p<0.01$; and ***= $p<0.001$.

782

783 **Figure 6: Glutamatergic, GABAergic, and glycinergic neurons in the sacral cord of intact and**
784 **spinal cord injured, antibody treated rats at 28 days after injury**. **a-e.** Representative
785 images of fluorescent in-situ hybridization for mRNA of **a.** glycine transporter 2 ($GlyT_2$), **b.**
786 glutamic acid decarboxylase 2 (GAD_2), and **c.** vesicular glutamate transporter 2 ($vGlut_2$). **d.**
787 Sections were counterstained with DAPI. **e.** Representative image of the three merged
788 probes, indicating the three analyzed regions *Laminae I-III*, *IV-V*, and *X*. **f-h.** quantification of
789 **f.** glycinergic, **g.** GABAergic, and **h.** glutamatergic neurons in the sacral cord of intact animals,
790 incomplete spinal cord injured animals treated with control antibody (Ctr Ab), and
791 incomplete spinal cord injured animals treated with anti-Nogo-A antibodies (anti-Nogo-A).
792 Data are presented as means ± SD. Scale bar is 20 μm in **a-d.**, and 300 μm in **e.**; ns = not
793 significant; *= $p<0.05$

794

795 **Figure 7: Spinal cord lesion assessment and distribution among groups: a.** Schematic
796 reconstruction of a spinal cord lesion. **b.** Representative Nissl staining of a spinal cord used

to reconstruct the lesion size. **c.** Neurofilament-160 immunohistological staining shows a high degree of correlation with the Nissl staining. **d.** Distribution of lesion sizes across the different animals. **e.** Comparison of the spared white matter between animals with a spinal cord injury group and no treatment (SCI only), spinal cord injured rats treated with control antibody (Ctr Ab), and spinal cord injured animals treated with anti-Nogo-A antibody (anti-Nogo-A) in case of a complete (black) or incomplete (gray) lesion. Data in e. are shown as median and 10-90 percentile.

Figure 1

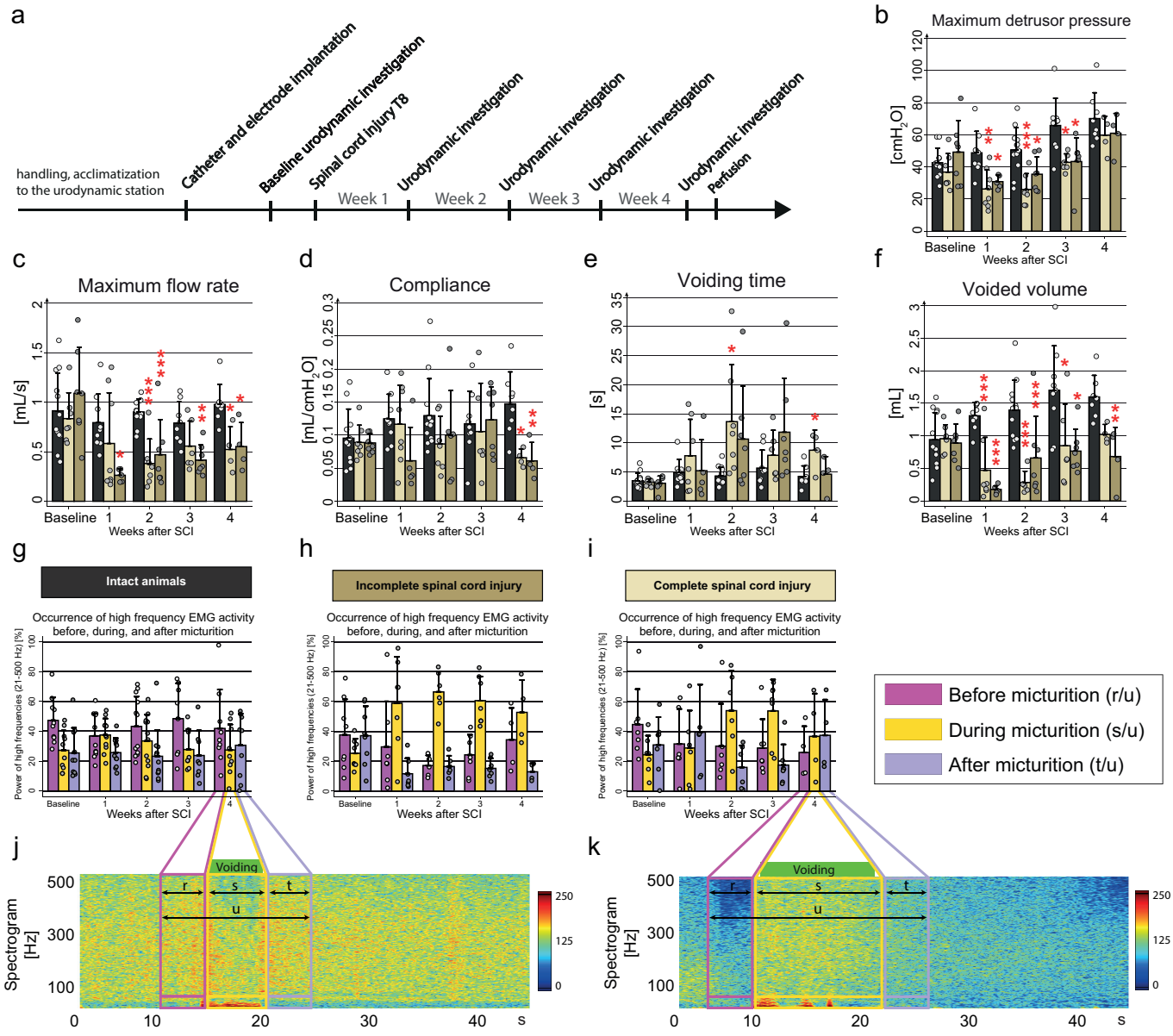

Figure 2

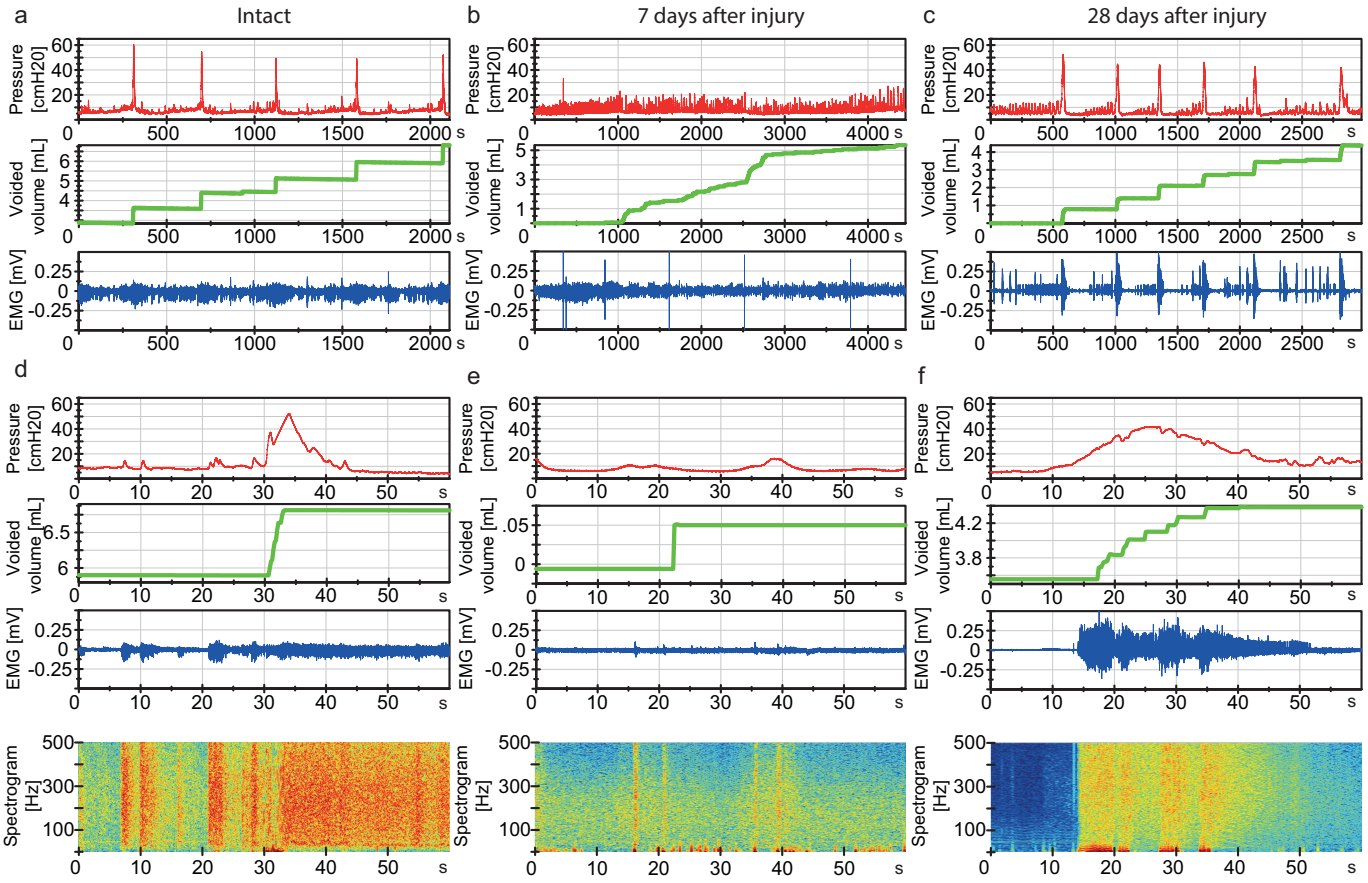

Figure 3

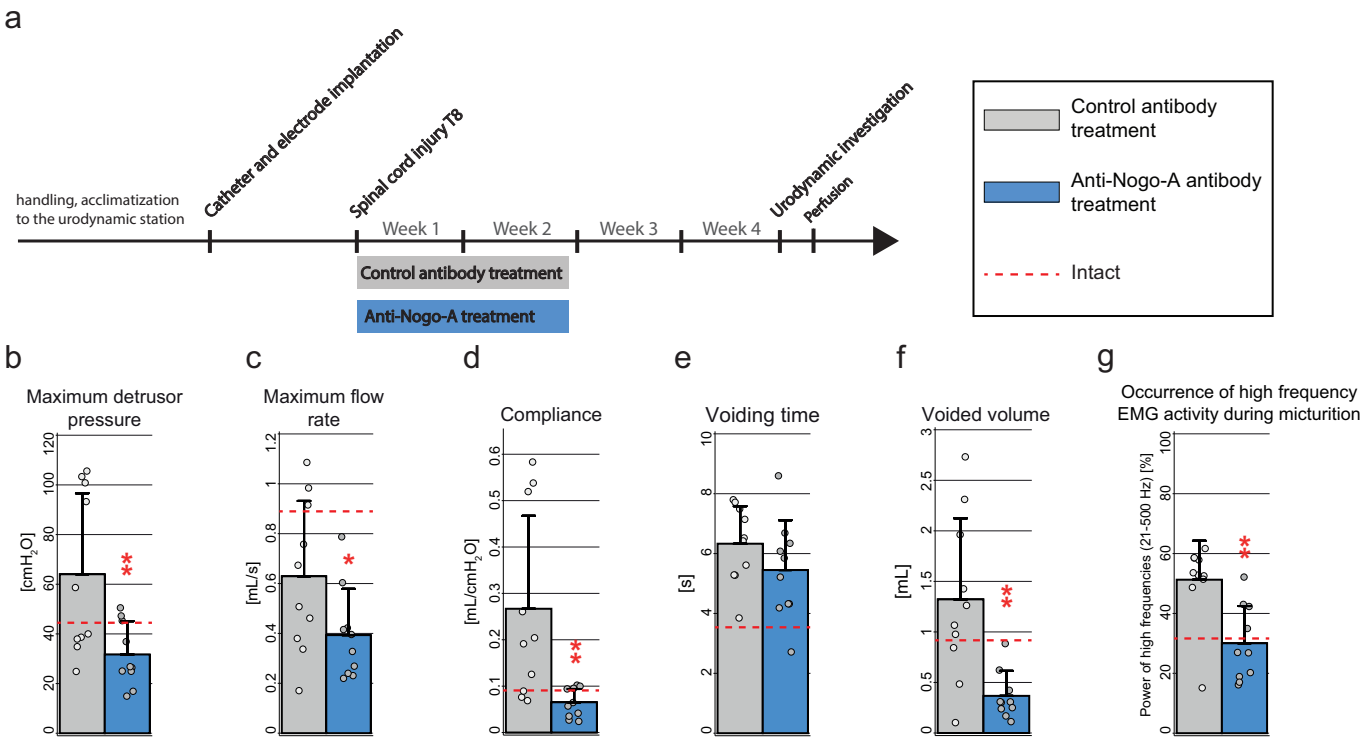

Figure 4

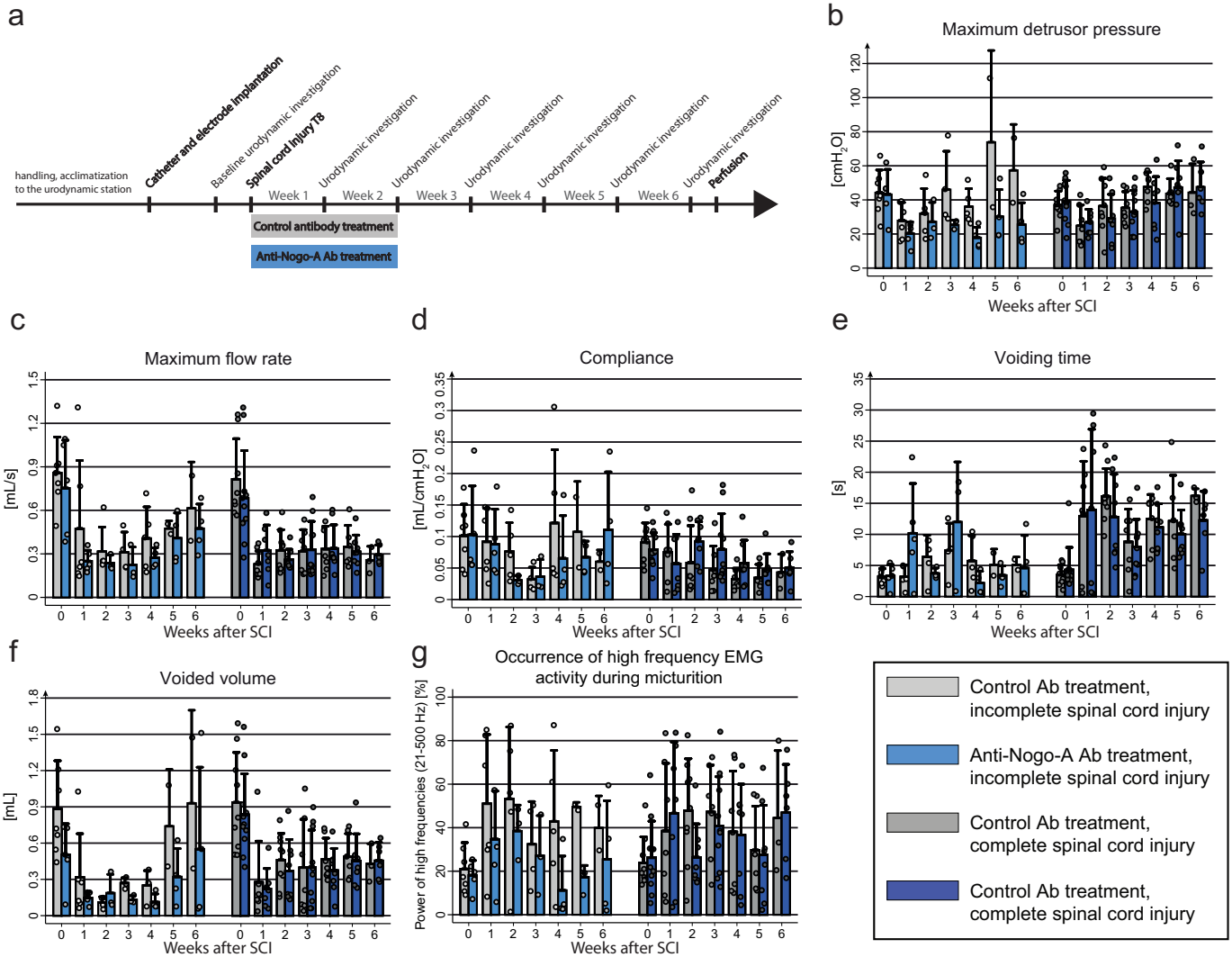

Figure 5

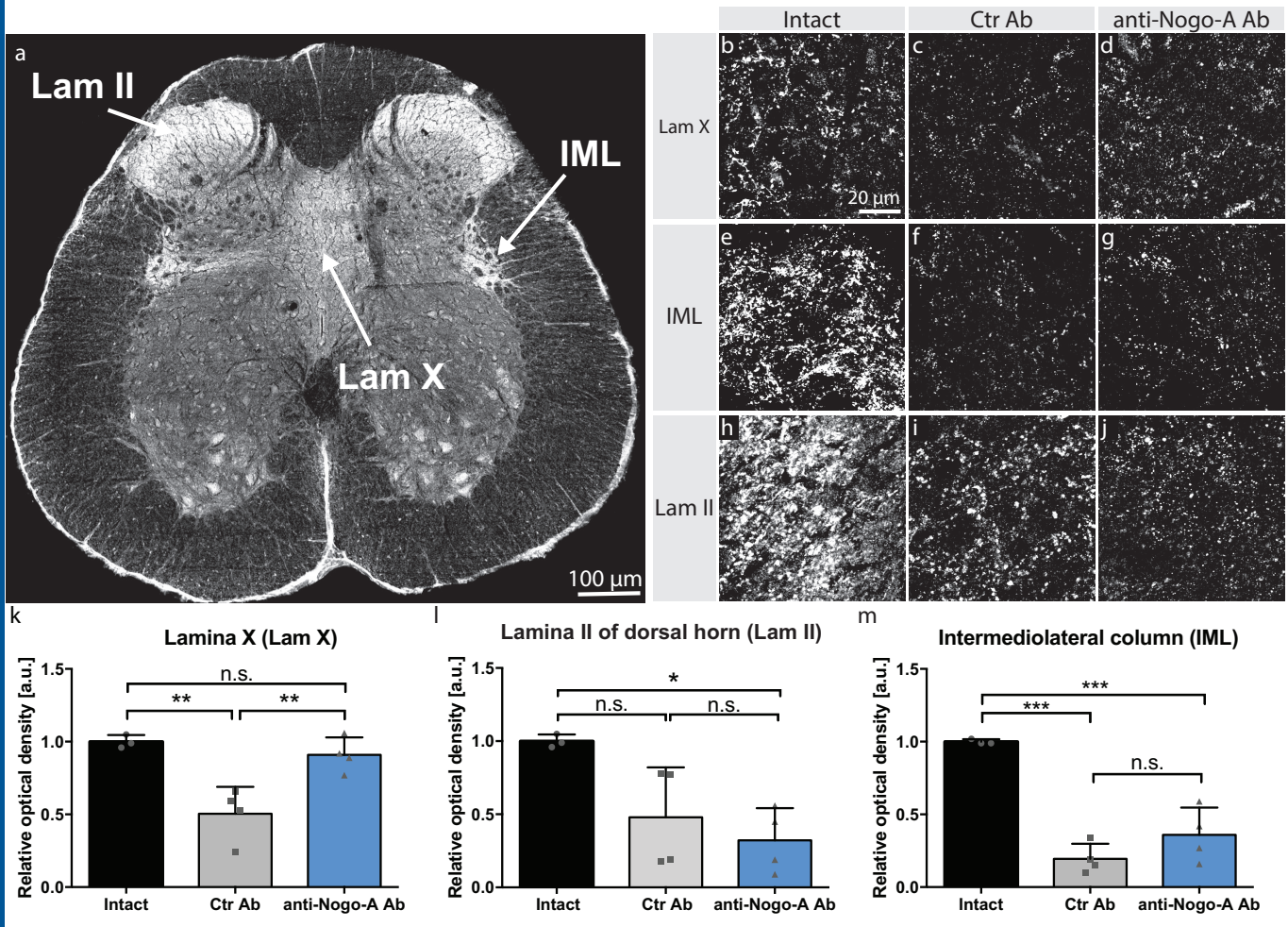

Figure 6

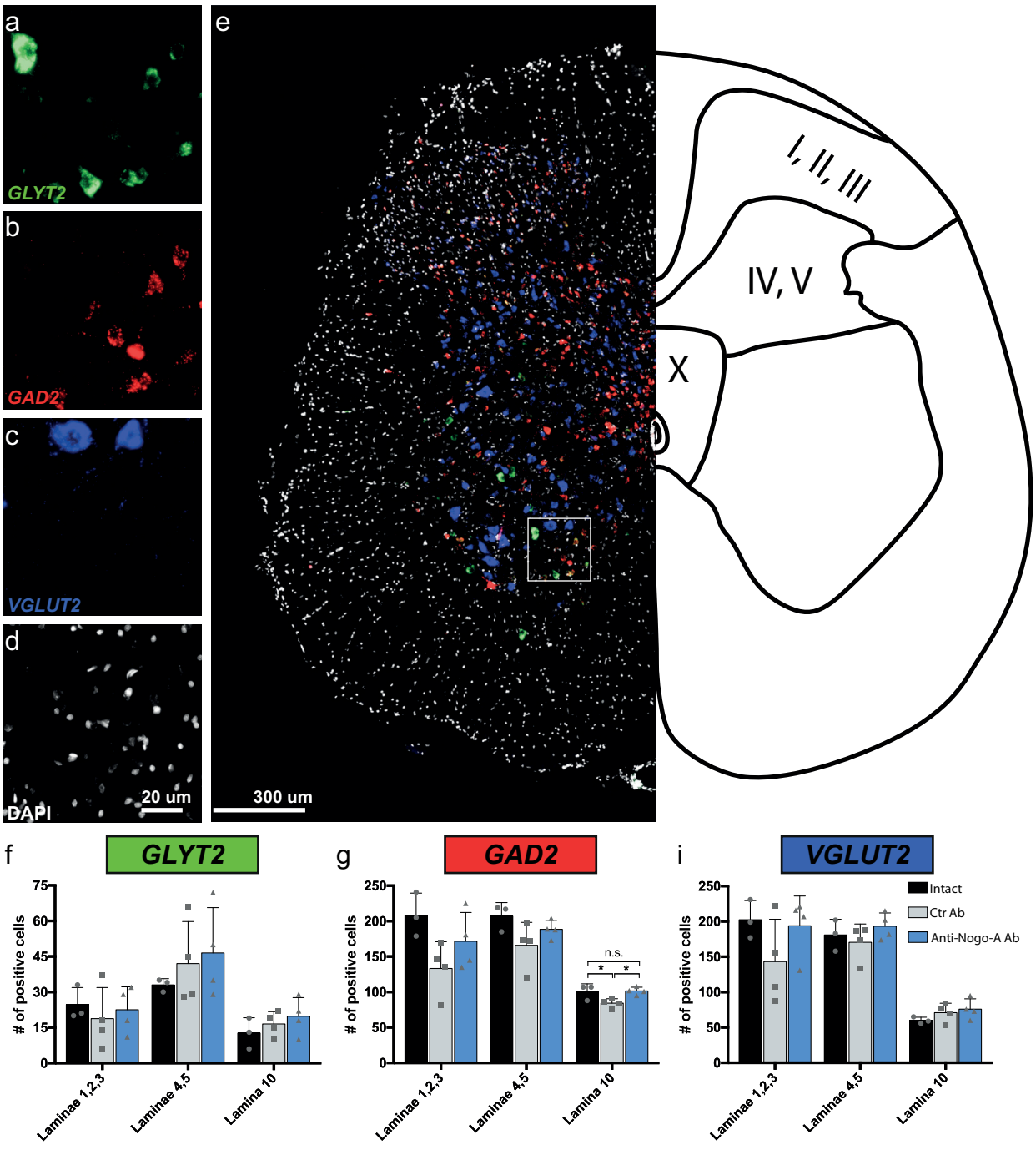

Figure 7